LUND UNIVERSITY

Radiative lifetimes and Lande factors of Rydberg 6pnp and 6pnf states of PbI by multichannel-quantum-defect theory

Dai, ZW; Li, Zhongshan; Zhankui, J

Link to publication

Radiative lifetimes and Landé factors of Rydberg $6pnp$ and $6pnf$ states of Pb I by multichannel-quantum-defect theory

Zhenwen Dai

Department of Physics, Jilin University, Changchun 130023, People's Republic of China

Z. S. Li

Department of Physics, Lund Institute of Technology, P.O. Box 118, S-221 00 Lund, Sweden

Jiang Zhankui

Department of Physics, Jilin University, Changchun 130023, People's Republic of China

Multichannel-quantum-defect theory analyses of $J=0$, 1, and 2 even-parity Rydberg series $6pnp$ and $6pnf$ of neutral lead have been performed for the experimental energy levels. The channel admixture coefficients were deduced and used to evaluate theoretical lifetimes and Landé (g_J) factors. Lifetime and g_J values for higher-lying excited states have also been predicted.

I. INTRODUCTION

The investigations on atomic Rydberg states remain an active research topic in the areas of atomic physics and laser spectroscopy [1]. MQDT (multichannel-quantum-defect theory) has been applied extensively to the description of perturbed Rydberg series of atoms [2–7]. Previously, most studies of Rydberg series focused on atoms possessing Rydberg states composed of an *s*-electron ion core and a highly excited electron [5–7]. However, in the present study of neutral lead, the Rydberg states consist of a *p*-electron ion core and a highly excited electron; the ion core ($6s^2 6p$) splits into the levels $^2P_{1/2}^0$ (lower ionization limit) and $^2P_{3/2}^0$ (upper ionization limit). The orbital-spin coupling in the lead atom is strong enough that the ground configuration ($6p^2$) and excited configurations $6pns$ and $6pnp$ are adequately described by jj coupling, while the configurations with a high angular-momentum electron (e.g., $6pnd, 6pnf$) are close to jK coupling. Moreover, lead is a high-Z atom where strong configuration interaction and channel mixing effects exist. The research on high-lying states of the carbon group is also useful in other subjects such as astrophysics and chemical reaction dynamics [8,9]. For the reasons mentioned above, it is of interest to investigate the Rydberg states of this kind of atom not only in theory but also in practice.

The energy positions of the Pb I odd-parity and even-parity Rydberg states have been determined using conventional absorption and emission spectroscopy [10,11] and laser spectroscopy [9,12–15]. In order to obtain a more clear insight into the properties of Rydberg states of Pb I, additional physical quantities such as radiative lifetimes and Landé (g_J) factors are required. Since the resonant lines of Pb I lie in the uv and vacuum uv regions, selective excitation and detection are rather difficult, and only a limited number of experimental lifetimes and g_J factors of lower energy levels have been measured using different techniques [16–20]. To make systematic investigations on even-parity Pb I Rydberg series, we recently performed lifetime and g_J factor

measurements on the $6pnd$ and $6pnf$ Rydberg states of Pb I by means of time-resolved laser spectroscopy [21]. In this paper, we use MQDT analyses of our measured lifetimes and g_J factors for a deeper understanding of the Rydberg state's features of this kind of atom testing MQDT theory. When more than one channel converged to a given limit, the MQDT wave functions derived from energy values are not sufficient to interpret g_J factors, hyperfine structures, etc.; therefore, a modified MQDT wave function is needed. In Sec. II the basic principles of MQDT and theoretical methods for calculating the lifetime and g_J factor of atomic Rydberg state are recalled. The theoretical results and analyses of lifetime values and g_J factors for the Rydberg series studied are given in Secs. III and IV. A final conclusion is provided in Sec. V.

II. BASIC THEORIES AND FORMULAS

Detailed descriptions of MQDT can be found in many papers as mentioned in Sec. I. Here only a brief description of the basic principles of MQDT and the theoretical methods for calculating lifetime and Landé factor of Rydberg state are presented.

The discrete energy levels E of a highly excited atom can be expressed by the Rydberg formula

$$E = I_i - \frac{R}{\nu_i^2} = I_j - \frac{R}{\nu_j^2}, \tag{1}$$

where I_i and ν_i are the *i*th ionization limit and the corresponding effective quantum number, respectively, and R is the mass-corrected Rydberg constant. The interaction between the excited electron and the ion core is separated into two regions: (I) $r > r_0$ (r_0 is the radius of the ion core); (II) $r < r_0$. The interaction in region I is Coulombic and described by the collision channels (*i* channel) identified in jj coupling, while the interaction in region II is non-Coulombic and described by the eigenchannels (α channels). The two kinds of channel are connected by an orthogonal transforma-

TABLE I. Theoretical and experimental lifetimes and g_J factors for $6pnp$ ($n=7-16$) series of Pb I.

Level	E_{expt} [15] (cm^{-1})	Lifetime (ns)			g_J factor	
		MQDT	Expt. [21]	HFR [20]	MODT	Expt. [21]
$7p(1/2,1/2)_1$	42 918.643[a]	95.9			0.7033	0.719(8)[e]
$7p(1/2,1/2)_0$	44 401.13	48.6		52.85		
$7p(1/2,3/2)_1$	44 674.9859[a]	40.7			1.4557	1.467(2)[e]
$7p(1/2,3/2)_2$	44 810.01	37.8			1.1364	1.170(2)[e]
$8p(1/2,1/2)_1$	51 320.598[a]	260.5			0.7134	0.673(4)[e]
$8p(1/2,1/2)_0$	51 781.02	129.9	130[d]	111.8		
$8p(1/2,3/2)_1$	51 911.19	105.4			1.4788	1.475(6)[e]
$8p(1/2,3/2)_2$	51 938.63	108.4	122(8)[d]	131.4	1.1553	1.156(6)[e]
$5f1/2[5/2]_2$	52 841.82[a]	56.7			0.8975	
$9p(1/2,1/2)_1$	54 653.72[a]	521.7	449(23)	583.4	0.7190	0.6772
$9p(1/2,1/2)_0$	54 861.81	262.0	274(12)	198.7		
$9p(1/2,3/2)_1$	54 928.0835[a]	213.4	237(11)	299.8	1.4848	1.4797(14)
$9p(1/2,3/2)_2$	54 929.57	236.1	240(10)	292.0	1.1611	1.1610(9)
$6f1/2[5/2]_2$	55 360.077[a]	104.7	104(8)		0.8961	0.8901(30)
$10p(1/2,1/2)_1$	56 338.932[a]	749.5	778(70)	976.0	0.7419	0.6976(30)
$10p(1/2,1/2)_0$	56 450.77	448.8	430(18)	325.6		
$10p(1/2,3/2)_2$	56 467.63	337.3	335(10)	405.0	1.1624	1.1616(4)
$10p(1/2,3/2)_1$	56 475.35	344.7	380(15)	373.7	1.4688	1.1421(3)
$7f1/2[5/2]_2$	56 719.794[a]	157.0	155(6)		0.8993	0.8990(20)
$7p(3/2,1/2)_1$	57 010.16	94.3	55(3)		1.1719	1.1740(20)
$11p(1/2,3/2)_2$	57 260.668[a]	77.0		181.7	1.1635	
$11p(1/2,1/2)_1$	57 317.841[a]	946.5	980(80)	1271.0	0.6880	0.6501
$11p(1/2,1/2)_0$	57 381.06	680.7	692(30)	458.6		
$11p(1/2,3/2)_1$	57 430.27	466.9	370(18)	170.5	1.4838	1.5010(9)
$8f1/2[5/2]_2$	57 497.795[a]	141.4	158(5)		1.0766	1.1044(12)
$7p(3/2,1/2)_2$	57 598.65	139.3	146(7)		1.0239	0.9960(30)

tion matrix $U_{i\alpha}$. To ensure correct asymptotic behavior of the wave functions for discrete levels, the following condition is required:

$$\det|U_{i\alpha}\sin\pi(\nu_i+\mu_\alpha)|=0, \tag{2}$$

where μ_α is the eigenquantum defect of eigenchannel α.

For a Rydberg series of configurations involving M interacting channels and N relevant series limits, there are $N-1$ independent equations similar to Eq. (1), and each equation determines a line L in the N-dimensional space of ν_i. Equation (2) describes a surface S in the same space. Since each bound state simultaneously satisfies Eqs. (1) and (2), the state energy can be calculated from the intersections of L and S. μ_α and $U_{i\alpha}$ are essential MQDT parameters. In MQDT analyses, the theoretical energy levels are fitted to the experimental ones by adjusting these parameters. It is very convenient for solving the problem to introduce an intermediate basis of pure-coupled channels $\bar{\alpha}$, and express $U_{i\alpha}$ as

$$U_{i\alpha}=\sum_{\bar{\alpha}}U_{i\bar{\alpha}}V_{\bar{\alpha}\alpha}, \tag{3}$$

where $U_{i\bar{\alpha}}$ is the transformation matrix between channels i and $\bar{\alpha}$, and can be obtained analytically from the 6-j symbols

[22]; $V_{\bar{\alpha}\alpha}$ is an orthogonal matrix generated by $M(M-1)/2$ successive rotations θ_{ij} becoming MQDT parameters instead of $U_{i\alpha}$ [4]. μ_α and θ_{ij} are slowly varying functions of energy. In this paper, the energy dependence of μ_α is considered by $\mu_\alpha=\mu_\alpha^0+\varepsilon\mu_\alpha^1$, where $\varepsilon=(I_i-E)/R$. The energy dependence of θ_{ij} is neglected as done in general. The optimal MQDT parameters are obtained by the nonlinear minimization method.

The MQDT wave function Ψ_n at the nth level can be expressed by the expansion of the wave functions Ψ_i of collision channels,

$$\Psi_n=\sum_i Z_i^{(n)}\Psi_i, \tag{4}$$

where $Z_i^{(n)}$ is the admixture coefficient of the i channel and is given by

$$Z_i^{(n)}=(-1)^{l+1}(\nu_i^{(n)})^{3/2}\sum_\alpha U_{i\alpha}\cos(\nu_i^{(n)}+\mu_\alpha)A_\alpha^{(n)}/N_n, \tag{5}$$

where $A_\alpha^{(n)}$ is the eigenchannel expansion coefficient and N_n is a normalization factor.

TABLE I. (*Continued*).

| Level | E_{expt} [15] (cm^{-1}) | Lifetime (ns) | | | g_J factor | |
		MQDT	Expt. [21]	HFR [20]	MODT	Expt. [21]
$12p(1/2,1/2)_1$	57 916.086[a]	709.6			0.7109	
$12p(1/2,1/2)_0$	57 968.05	932.6	930			
$12p(1/2,3/2)_1$	57 993.98	716.4	650(50)		1.4981	1.4930(9)
$12p(1/2,3/2)_2$	58 008.62	502.0	490(20)		1.1572	1.1731(5)
$9f1/2[5/2]_2$	58 095.3[b]	358.5			0.9263	
$7p(3/2,3/2)_1$	58 324.46	77.6	103(5)		1.1705	1.1430(20)
$13p(1/2,3/2)_2$	58 397.77	748.0	750(100)		1.1615	1.1724(20)
$13p(1/2,1/2)_1$	58 369.38[c]	58.4			1.5195	
$13p(1/2,1/2)_0$	58 383.94	1168.3				
$13p(1/2,3/2)_1$	58 402.61	308.1	100(7)		1.4864	1.6109(9)
$10f1/2[5/2]_2$	58 455.6[b]	462.7			0.9210	
$14p(1/2,1/2)_1$	58 637.60[c]	801.6			0.8146	
$14p(1/2,1/2)_0$	58 654.15	1352.9				
$14p(1/2,3/2)_1$	58 669.71	1071.8	1200		1.4768	1.5216(9)
$14p(1/2,3/2)_2$	58 666.67	550.3			1.1614	1.1712(9)
$11f1/2[5/2]_2$	58 714.2[b]	498.3			0.9311	
$15p(1/2,1/2)_1$	58 852.19[f]	1037.3			0.7440	
$15p(1/2,3/2)_2$	58 849.8[b]	128.1			1.1605	1.1798(20)
$15p(1/2,1/2)_0$	58 861.90	1464.9				
$15p(1/2,3/2)_1$	58 872.56	1308.5	1300		1.4928	1.5133(9)
$12f1/2[5/2]_2$	58 905.4[b]	301.2			0.9949	
$7p(3/2,3/2)_2$	58 971.32	34.6			1.1671	
$16p(1/2,1/2)_1$	59 008.72[f]	182.6			0.7456	
$16p(1/2,1/2)_0$	59 016.34	1501.0				
$16p(1/2,3/2)_1$	59 024.27	375.4			1.5043	1.5114(20)
$16p(1/2,3/2)_2$	59 041.46	268.1			1.1627	1.0936(50)

[a]Experimental levels from Wood and Andrew [11].
[b]Experimental levels from Ding *et al.* [9].
[c]Experimental levels from Farooqi *et al.* [13].
[d]Measured lifetimes from Gorshov and Verolainen [17].
[e]Measured Landé factors from Wood and Andrew [19].
[f]MQDT theoretical levels obtained by us.

Utilizing MQDT wave functions, the lifetime of Rydberg levels can be predicted by using the parametric theory [23]. Because M interacting channels consist of the perturbing channels and the perturbed channels, from Eq. (4) the wave function can be rewritten as

$$\Psi_n = \sum_a Z_a^{(n)} \Psi_a + \sum_b Z_b^{(n)} \Psi_b, \qquad (6)$$

where Ψ_a and Ψ_b are the perturbed and perturbing channel wave functions, respectively. In the electric dipole radiation approximation, the radiative decay rate Γ_n of the level n can be given by

$$\Gamma_n = \sum_a (Z_a^{(n)})^2 \Gamma_a + \sum_b (Z_b^{(n)})^2 \Gamma_b, \qquad (7)$$

where Γ_a and Γ_b are the decay rates of pure Rydberg levels that are expected to be proportional to $1/(\nu^{(n)})^3$ [23]. In gen-

eral, as the coefficients $Z_b^{(n)}$ have considerable values only for the levels near the perturbers, the variation of Γ_n with $\nu_b^{(n)}$ can be neglected. Thus, Γ_n can be expressed as

$$\Gamma_n = \sum_a (Z_a^{(n)})^2 \frac{\gamma_a}{(\nu_a^{(n)})^3} + \sum_b (Z_b^{(n)})^2 \Gamma_b, \qquad (8)$$

where γ_a and Γ_b are lifetime parameters relevant to the perturbed channels and perturbing channels, respectively, and are not dependent on the level n. The lifetime τ_n of the level n can be calculated from the radiative decay rate Γ_n as $\tau_n = 1/\Gamma_n$. The parameters γ_a and Γ_b can be determined by fitting theoretical lifetimes to the experimental values with the admixture coefficients obtained from MQDT analyses.

Using MQDT wave functions, the Landé factor $g_J^{(n)}$ of the level n can be calculated by the expression

$$g_J^{(n)} = \sum_a (Z_a^{(n)})^2 g_J(a) + \sum_b (Z_b^{(n)})^2 g_J(b), \qquad (9)$$
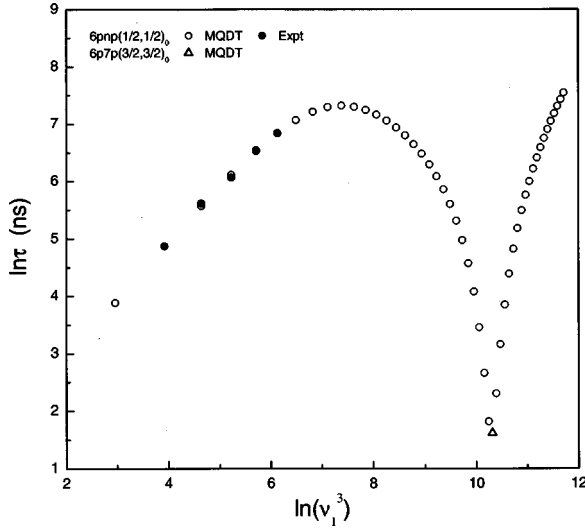
FIG. 1. Lifetimes calculated by MQDT and comparison with previous experimental values for $J=0$ even-parity levels.

where g_J (*a*) and g_J (*b*) are the Landé factors of the perturbed and perturbing channels, respectively, which can be calculated analytically in the pure-coupling representations of the corresponding channels. From previous MQDT analyses [3,24–26], it is known that energy data do not contain sufficient information to describe the properties of Rydberg levels and to get all the MQDT parameters for determining factual MQDT wave functions. When more than one channel converged to an ionization limit, the θ angles, describing the orthogonal transformation of these degenerate channels, have no effect on theoretical energies. This will lead to an uncertainty in the wave functions obtained by energy fitting. Lifetimes of Rydberg levels are generally insensitive to this uncertainty, whereas g_J factors are very sensitive to it. Therefore, g_J factors rather than lifetime values can be used to optimize these special θ angles to improve MQDT wave functions through getting a new set of $Z_i^{(n)}$.

In principle, it is needed to perform improvement of wave functions by optimizing the special θ angles mentioned above belonging to not only perturbed channels but also to perturbing channels. However, the coupling schemes of perturbing channels are usually the intermediate couplings, and g_J factor values of these channels are difficult to know. So it is very convenient to take g_J factors [g_J (*b*) in Eq. (9)] of perturbing channels as fitting parameters. The intermediate coupling information of perturbing channels as well as the available modification of MQDT wave function from g_J fitting are contained in these g_J optimal parameters. g_J (*a*) in Eq. (9) is still the analytical Landé factor of the perturbed channel in pure-coupling schemes.

III. THEORETICAL RESULTS AND ANALYSES OF LIFETIMES

The configuration of $J=0$ even-parity Rydberg series of Pb I is $6pnp$ and it consists of two channels: $6pnp(1/2,1/2)_0$ and $6pnp(3/2,3/2)_0$, which converge to the first ionization limit $^2P_{1/2}$ (59 819.57 cm^{-1}) and the second one $^2P_{3/2}$

(73 900.64 cm^{-1}), respectively. Using experimental energy levels $6pnp(1/2,1/2)_0$ ($n=7-50$) and $6p7p(3/2,3/2)_0$ reported by Hasegawa and Suzuki [15], we made MQDT calculations and obtained MQDT parameters and wave functions of $J=0$ even-parity states. From Eq. (8), the radiative decay rate for these levels is given as

$$\Gamma_n = (Z_{(1/2,1/2)_0}^{(n)})^2 \frac{\gamma}{(\nu_1^{(n)})^3} + (Z_{(3/2,3/2)_0}^{(n)})^2 \Gamma_{(3/2,3/2)_0}, \quad (10)$$

where γ and $\Gamma_{(3/2,3/2)_0}$ are the lifetime parameters of the $6pnp(1/2,1/2)_0$ and $6pnp(3/2,3/2)_0$ channels, $\nu_1^{(n)}$ is the effective quantum number in the first limit. Using the nonlinear minimization method, we fitted the theoretical lifetimes to the experimental values [21,17] with the MQDT admixture coefficients and obtained the lifetime parameters $\gamma = 3.765 \times 10^8$ s^{-1}, $\Gamma_{(3/2,3/2)_0} = 7.406 \times 10^8$ s^{-1}. The calculated and measured lifetimes of the $6pnp(1/2,1/2)_0$ levels ($7 \leq n \leq 16$) are compared in Table I together with some previous theoretical results by the relativistic Hartree-Fock (HFR) method [20]. Lifetime calculations for the even-parity $6pnp$ $J=0$ levels have been extended up to the state $6p50p$ $(1/2,1/2)_0$ at 59 766.65 cm^{-1} as shown in Fig. 1. There are obvious decreases of the predicted lifetimes around $\nu_1 = 30.4$ due to perturbation of the $6p7p(3/2,3/2)_0$ state.

For $J=1$ even-parity Rydberg configurations of Pb I including $6pnp$ and $6pnf$, the collision channels are labeled as

$6pnp$	$6pnp$	$6pnp$	$6pnp$	$6pnf$
$(\frac{1}{2},\frac{1}{2})_1$	$(\frac{1}{2},\frac{3}{2})_1$	$(\frac{3}{2},\frac{3}{2})_1$	$(\frac{3}{2},\frac{1}{2})_1$	$\frac{3}{2}[\frac{3}{2}]_1$

There are 30 experimental levels of $J=1$ even-parity available in the literature [11,13,15]. Our MQDT analyses are performed with these experimental levels. The radiative decay rate for $J=1$ even-parity Rydberg series can be expressed as

$$\Gamma_n = (Z_{(1/2,1/2)_1}^{(n)})^2 \frac{\gamma_1}{(\nu_1^{(n)})^3} + (Z_{(1/2,3/2)_1}^{(n)})^2 \frac{\gamma_2}{(\nu_1^{(n)})^3}$$
$$+ (Z_{(3/2,3/2)_1}^{(n)})^2 \Gamma_{(3/2,3/2)_1} + (Z_{(3/2,1/2)_1}^{(n)})^2 \Gamma_{(3/2,1/2)_1}$$
$$+ (Z_{3/2[3/2]_1}^{(n)})^2 \Gamma_{3/2[3/2]_1}. \quad (11)$$

By fitting the theoretical lifetimes to the experimental values [21] with the MQDT wave functions, we obtained the lifetime parameters: $\gamma_1 = 1.667 \times 10^8$ s^{-1}, $\gamma_2 = 5.007 \times 10^8$ s^{-1}, $\Gamma_{(3/2,3/2)} = 0.334 \times 10^8$ s^{-1}, $\Gamma_{(3/2,1/2)_1} = 0.115 \times 10^8$ s^{-1}, and $\Gamma_{3/2[3/2]_1} = 1.451 \times 10^8$ s^{-1}. The calculated and measured lifetimes of the $J=1$ even-parity Rydberg $6pnp$ levels ($7 \leq n \leq 16$) are listed in Table I and the predicted MQDT lifetimes of the $J=1$ even-parity states up to $6p27p$ $(\frac{1}{2},\frac{3}{2})_1$ at 59 607.94 cm^{-1} are shown in Fig. 2. The decreases of lifetimes in three regions of ν_1 are due to the stronger perturbations of the perturbers $6p7p$ $(\frac{3}{2},\frac{1}{2})_1$, $6p7p$

$(\frac{3}{2},\frac{3}{2})_1$, and $6p5f\ \frac{3}{2}[\frac{3}{2}]_1$. In our MQDT analyses, the level $6p13p\ (\frac{1}{2},\frac{1}{2})_1$ is higher than $6p13p\ (\frac{1}{2},\frac{3}{2})_1$. The level $6p13p\ (\frac{1}{2},\frac{1}{2})_1$ is near the perturber $6p7p\ (\frac{3}{2},\frac{3}{2})_1$. In our theoretical analyses, it is found that the MQDT lifetimes and g_J factors of the $J=1$ series are more consistent with the experimental values when $6p13p\ (\frac{1}{2},\frac{1}{2})_1$ was fitted to be higher than $6p13p\ (\frac{1}{2},\frac{3}{2})_1$ in energy fitting. The only measurement for the energy of $6p13p\ (\frac{1}{2},\frac{1}{2})_1$ was done through an identification of a very weak ionization signal by the group of Farooq et al. [13], which is 58 369.38 cm^{-1} and lower than $6p13p\ (\frac{1}{2},\frac{3}{2})_1$. We think that the position of $6p13p\ (\frac{1}{2},\frac{1}{2})_1$ needs to be identified more reliably by experiment.

The $J=2$ even-parity Rydberg series can be described by six collision channels, which are conventionally labeled as

$6pnp$	$6pnf$	$6pnp$	$6pnf$	$6pnf$	$6pnp$
$(\frac{1}{2},\frac{3}{2})_2$	$\frac{1}{2}[\frac{5}{2}]_2$	$(\frac{3}{2},\frac{3}{2})_2$	$\frac{3}{2}[\frac{3}{2}]_2$	$\frac{3}{2}[\frac{5}{2}]_2$	$(\frac{3}{2},\frac{1}{2})_2$

The radiative decay rate for $J=2$ even-parity Rydberg series has the form

$$\Gamma_n = (Z^{(n)}_{(1/2,3/2)_2})^2 \frac{\gamma_1}{(\nu_1^{(n)})^3} + (Z^{(n)}_{1/2[5/2]_2})^2 \frac{\gamma_2}{(\nu_1^{(n)})^3}$$
$$+ (Z^{(n)}_{(3/2,3/2)_2})^2 \Gamma_{(3/2,3/2)_2} + (Z^{(n)}_{3/2[3/2]_2})^2 \Gamma_{3/2[3/2]_2}$$
$$+ (Z^{(n)}_{3/2[5/2]_2})^2 \Gamma_{3/2[5/2]_2} + (Z^{(n)}_{(3/2,1/2)_2})^2 \Gamma_{(3/2,1/2)_2}.$$

(12)

In our MQDT calculations, most of the experimental energy levels of the $J=2$ even-parity states as high as $6p55p\ (\frac{1}{2},\frac{3}{2})_2$ at 59 775.51 cm^{-1} can be obtained from the measurement by Hasegawa and Suzuki [15]. The other unmeasured levels under the $6p55p\ (\frac{1}{2},\frac{3}{2})_2$ state in Ref. [15] can be supplemented from [9,11,12]. Utilizing the same procedure as above, the parameters: $\gamma_1=2.765\times10^8$ s^{-1}, $\gamma_2=10.152 \times10^8$ s^{-1}, $\Gamma_{(3/2,3/2)_2}=0.510\times10^8$ s^{-1}, $\Gamma_{3/2[3/2]_2}=0.032 \times10^8$ s^{-1}, $\Gamma_{3/2[5/2]_2}=115.734\times10^8$ s^{-1}, and $\Gamma_{(3/2,1/2)_2} =0.254\times10^8$ s^{-1} are obtained. The theoretical and experimental lifetimes of the $J=2$ even-parity Rydberg levels $6pnp$ ($7\leqslant n\leqslant16$) and $6pnf\ \frac{1}{2}[\frac{5}{2}]_2$ ($5\leqslant n\leqslant12$) are presented in Table I and the calculated MQDT lifetimes of all the $J=2$ even-parity states under the $6p55p\ (\frac{1}{2},\frac{3}{2})_2$ state are shown in Fig. 3. There exist four perturbers $6p7p\ (\frac{3}{2},\frac{1}{2})_2$, $6p7p\ (\frac{3}{2},\frac{3}{2})_2$, $6p5f\ \frac{3}{2}[\frac{3}{2}]_2$, and $6p5f\ \frac{3}{2}[\frac{5}{2}]_2$ in the studied region of $J=2$ energy level, which cause distinct departure of lifetime from the Rydberg character of $(\nu_1)^3/\gamma_i$. It should be pointed out that the perturber level $6p5f\ \frac{3}{2}[\frac{5}{2}]_2$, which was not detected under the $6p55p\ (\frac{1}{2},\frac{3}{2})_2$ state by Hasegawa and Suzuki [15], has been determined by our MQDT analyses as shown in Fig. 3 for the last valley.
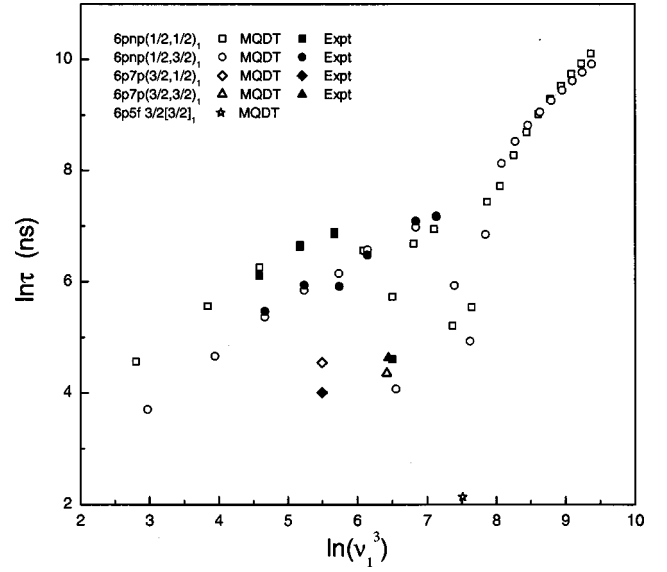

FIG. 2. Lifetimes calculated by MQDT and comparison with previous experimental values for $J=1$ even-parity levels.

As seen from Table I, HFR theoretical lifetimes have larger errors compared with our MQDT results because there exist a number of configuration interactions in the even-parity series that are difficult to consider very well in ab initio calculations of atomic structure. In the case of $J=1$ series, MQDT results have larger errors in contrast to the cases of $J=0$ and 2 series. The main reason for this may be that the fluorescence signals of $J=1$ levels are much weaker and bring larger measurement errors on the lifetimes and g_J factors of $J=1$ levels.

Moreover, for our MQDT calculations it will be valuable to give the root-mean-square (rms) deviation between the theoretical and experimental energy values. The rms for J
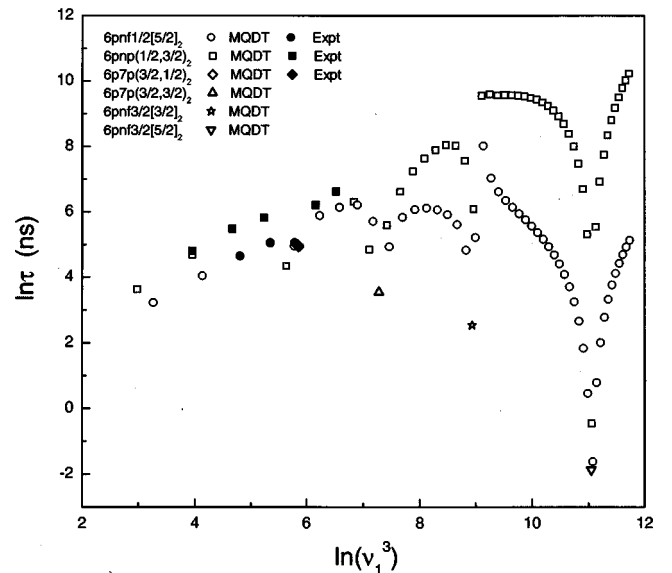

FIG. 3. Lifetimes calculated by MQDT and comparison with previous experimental values for $J=2$ even-parity levels.
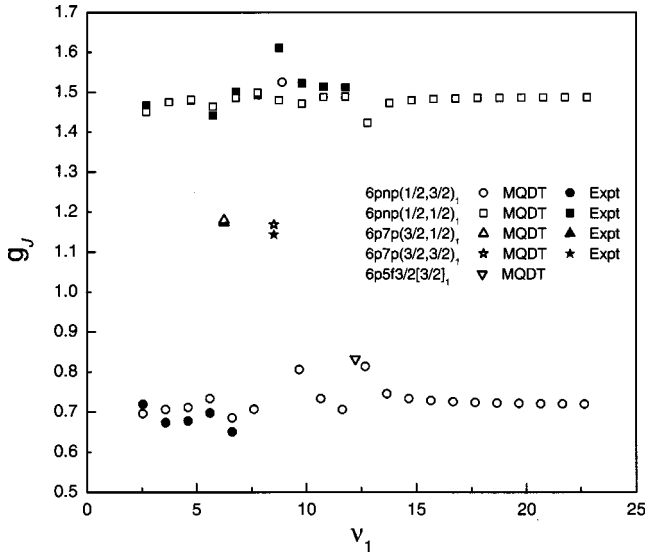
FIG. 4. Landé factors calculated by MQDT and comparison with previous experimental values for $J=1$ even-parity levels.

FIG. 5. Landé factors calculated by MQDT and comparison with previous experimental values for $J=2$ even-parity levels.

$=0$ levels is 24.49 cm^{-1}. If the lowest level $6p7d$ $(1/2,1/2)_0$ is excluded, the rms is 2.39 cm^{-1}. For $J=1$ levels the rms is 10.88 cm^{-1}, and when we exclude the $6p7d$ $(1/2,3/2)_1$ level having the largest theoretical deviation the rms is 7.27 cm^{-1}. The $J=2$ series has the smallest rms 1.95 cm^{-1} compared with other series.

IV. THEORETICAL RESULTS AND ANALYSES OF LANDÉ g_J FACTORS

In the $J=1$ even-parity Rydberg series of Pb I, the g_J factors of $6pnp$ $(\frac{1}{2},\frac{1}{2})_1$ and $6pnp$ $(\frac{1}{2},\frac{3}{2})_1$ under the pure coupling condition are 0.6667 and 1.5, respectively. With Eq. (9) and the $J=1$ MQDT wave functions, theoretical g_J are fitted to the experimental values measured by us [21] and the parameters are obtained: $g_J[(\frac{3}{2},\frac{3}{2})_1]=2.1365$, $g_J[(\frac{3}{2},\frac{1}{2})_1]$ $=1.1821$, $g_J[\frac{3}{2}[\frac{3}{2}]_1]=0.8530$, and $\theta=0.0647$ rad. The calculated and measured g_J of the $J=1$ even-parity $6pnp$ levels are listed in Table I and shown in Fig. 4 $(7\leqslant n\leqslant 27)$.

For the pure-coupling cases, the g_J factors of the $J=2$ states $6pnp$ $(\frac{1}{2},\frac{3}{2})_2$ and $6pnf$ $\frac{1}{2}[\frac{3}{2}]_2$ are 1.1667 and 0.8889, respectively. By the same procedure as above, the parameters and the θ angle: $g_J[(\frac{3}{2},\frac{3}{2})_2]=1.3038$, $g_J[\frac{3}{2}[\frac{3}{2}]_2]=1.0683$, $g_J[\frac{3}{2}[\frac{5}{2}]_2]=0.9128$, $g_J[(\frac{3}{2},\frac{1}{2})_2]=1.1823$, and θ $=-0.0945$ rad are found. Comparisons between the calculated and measured g_J factors of the $J=2$ even-parity states under $6p16p$ $(\frac{1}{2},\frac{3}{2})_2$ are given in Table I and the predicted g_J values of the $J=2$ even-parity states up to $6p55p$ $(\frac{1}{2},\frac{3}{2})_2$ are shown in Fig. 5.

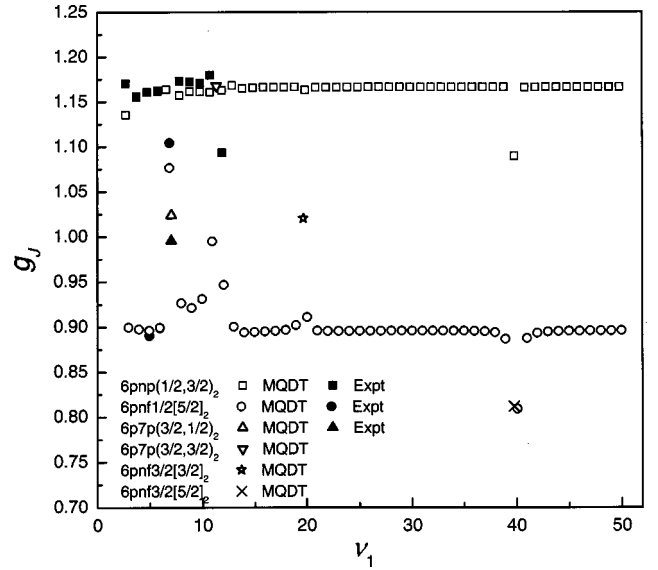As can be seen from Figs. 4 and 5, most of the g_J factors

are quite close to the corresponding g_J values of the assigned pure coupling schemes, which indicate that the coupling schemes assigned to most of studied channels are very good. It is also obvious that some g_J factors have been largely perturbed by the perturber levels just as the lifetime cases.

V. CONCLUSION

In conclusion, the MQDT analyses are carried out for the $J=0$, 1, and 2 even-parity Rydberg series levels of Pb I, and the MQDT wave functions of each level, i.e., channel admixture coefficients are obtained. With these wave functions and utilizing the experimental lifetimes and Landé (g_J) factors measured previously, the theoretical lifetimes of $J=0$, 1, and 2 levels are evaluated as well as the theoretical g_J factors of $J=1$ and 2 levels. A good overall agreement between the MQDT theoretical and experimental lifetimes and g_J factors has been achieved except for few levels of the $J=1$ series. In addition, the theoretical lifetimes calculated here by MQDT are better than those evaluated by the HFR method. Therefore, we can conclude that our MQDT analyses for $J=0$, 1, and 2 even-parity Rydberg series levels are reliable to evaluate the lifetimes and g_J factors of these series levels.

[1] M. Aymar, C. H. Greene, and E. Luc-Koenig, Rev. Mod. Phys. **68**, 1015 (1996).

[2] K. T. Lu and U. Fano, Phys. Rev. A **2**, 81 (1970).

[3] K. T. Lu, Phys. Rev. A **4**, 579 (1971).

[4] C. M. Lee and K. T. Lu, Phys. Rev. A **8**, 1241 (1973).

[5] M. Aymar and O. Robaux, J. Phys. B **12**, 531 (1979).

[6] J. A. Armstrong, P. Esherick, and J. J. Wynne, Phys. Rev. A **15**, 180 (1977).

[7] M. Aymar, A. Debarre, and O. Robaux, J. Phys. B **13**, 1089 (1980).

[8] D. M. Pyper and M. R. Hartoog, Astrophys. J. **198**, 555 (1975).

[9] D. Ding, M. Jin, H. Liu, and X. Liu, J. Phys. B **22**, 1979 (1989).

[10] C. M. Brown, S. G. Tilford, and M. L. Ginter, J. Opt. Soc. Am. **67**, 1240 (1977).

[11] D. R. Wood and K. L. Andrew, J. Opt. Soc. Am. **58**, 818 (1968).

[12] W. A. Young, M. Y. Mirza, and W. W. Duley, J. Phys. B **13**, 3175 (1980).

[13] S. M. Farooqi, M. Nawaz, S. A. Bhatti, M. Ahmad, and M. A. Baig, J. Phys. B **28**, 2875 (1995).

[14] S. Budick and J. Snir, Phys. Lett. A **24**, 689 (1967).

[15] S. Hasegawa and A. Suzuki, Phys. Rev. A **53**, 3014 (1996).

[16] T. Anderson, Nucl. Instrum. Methods **110**, 35 (1973).

[17] V. N. Gorshov and Ya F. Verolainen, Opt. Spectrosk. **58**, 1883 (1985) [Opt. Spectrosc. **58**, 848 (1985)].

[18] D. H. Giers, J. B. Atkinson, and L. Krause, Can. J. Phys. **62**, 1616 (1984).

[19] D. R. Wood, K. L. Andrew, A. Giacchetti, and R. D. Cowan, J. Opt. Soc. Am. **58**, 830 (1968).

[20] Z. S. Li, S. Svanberg, E. Biemont, P. Palmeri, and Jiang Zhankui, Phys. Rev. A **57**, 3443 (1998).

[21] Z. S. Li, Jiang Zhankui, U. Berzinsh, A. Persson, and S. Svanberg, J. Phys. B **34**, 3501 (2001).

[22] R. D. Cowan, *The Theory of Atomic Structure and Spectra* (University of California, Berkeley, 1981).

[23] M. Aymar, R. J. Champeau, C. Delsart, and J.-C. Keller, J. Phys. B **14**, 4489 (1981).

[24] P. Grafström, C. Levinson, H. Lundberg, S. Svanberg, P. Grundevik, L. Nilsson, and M. Aymar, Z. Phys. A **308**, 95 (1982).

[25] M. Aymar, J. Opt. Soc. Am. B **1**, 239 (1984).

[26] L. Xingye, L. Wanfa, J. Zhankui, and J. Larsson, Phys. Rev. A **49**, 4443 (1994).